



ISSN Print: 2394-7500
 ISSN Online: 2394-5869
 Impact Factor: 5.2
 IJAR 2019; 5(2): 261-263
www.allresearchjournal.com
 Received: 28-12-2018
 Accepted: 03-01-2019

Anshu Anand
 Research Scholar Department
 of Physics CCS University
 Meerut, Uttar Pradesh, India

Suspension Clogging

Anshu Anand

Abstract

The movement through a single constricted channel of a charged-stabilized suspension is experimentally analysed by independently monitoring the particles. Surprisingly, the conduct is observed to be qualitatively identical to that of dry granular inertial systems. For small values of the neck-to-particle size ratio ($D/d < 3$), clogs form randomly as arches of particle span the constriction. At the transition to a virtually uninterrupted flow, this especially small value of D/d is due to the low effective friction between the particles, accomplished by the functionalization and lubrication of the particle.

Keywords: Charged-stabilized suspension, neck-to-particle size ratio and lubrication

Introduction

Experience indicates that when the particles create a clog obstructing the path, solid particles pushed into a narrow constriction may either flow slowly, intermittently or not flow at all. In various devices involving particle accumulation or discharge, such as the hopper of an emptying granular silo, the hourglass collar, microfluidic and filtration loops where a filled liquid enters a computer or permeates a membrane, but also crowds of people who exit a room or a hungry herd entering a room through a door^[1-5]. Blockage of pipelines or channels is a natural occurrence that can occur in a wide variety of physicochemical and biological processes, such as pipeline transport of oil or coal in liquids, pipeline transport of wheat in silos, capillary viscometer colour coating, and cholesterol in human blood vessels. The blockage can be caused by two qualitatively distinct phenomena: jamming at high suspended particle densities and blockage due to increasing accumulated layers on the pipe. The flow channel is narrowed by particle accumulation on channel walls and nontrivial patterns such as meandering or necking of the remaining flow channel can occur. A typical example of a meandering pattern is that of rivers created by sedimentation of soil particles on slow stream riverbanks^[6-9]. In the examples mentioned above, it may be of fundamental importance to find a common physical process that drives the creation of patterns when they show different patterns, even though the physics involved might be somewhat similar. We developed a computational model in order to analyse the fundamental processes. This model should take as basic a form as possible, but it should also capture the processes in actual structures that are important. In our model, there are two competing mechanisms: particle deposition contributes to changes in local flow velocities, which may in turn allow deposited particles to be detached. In the models, the simplest possible laws of connection and detachment were applied and more complex mechanical relations between the particles and the flow were not taken into account. To obtain potential step boundaries, large device sizes and long runs were needed, and so we used two-dimensional simulations to get better accuracy. We used the lattice-Boltzmann approach described above to model the particle suspension channel movement.

Results and Discussion

The channel flow of suspension with deposition can be defined by only two parameters for a fixed number of particles. The solid volume fraction ϕ and the threshold τP . If τP is increased from zero at a constant ϕ , we find up to six distinct regimes in the behaviour of the suspension: ordinary pipe-flow ($\tau P \leq \tau d$), two types of deposition in the both meandering and necking regimes, and blocking (fig 1).

Correspondence Author:
Anshu Anand
 Research Scholar Department
 of Physics CCS University
 Meerut, Uttar Pradesh, India

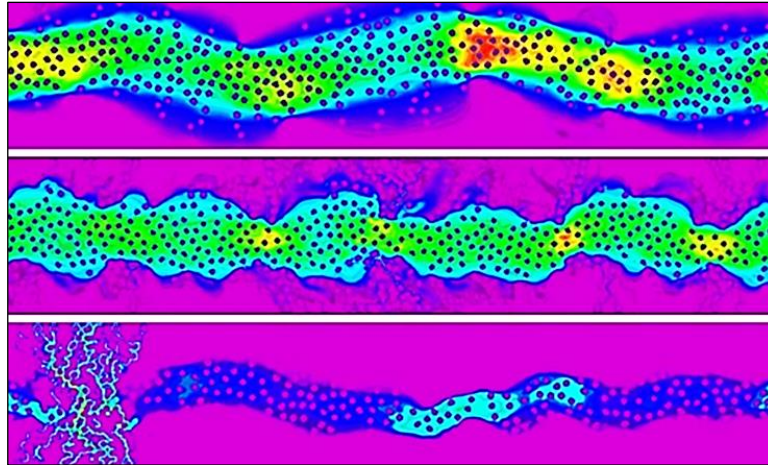


Fig 1: Snapshots with color coded fluid velocities (violet is zero velocity and red is high velocity). Meandering for $\tau P = 0.18$, $\phi = 0.26$, and $C_s = 0.11$. Necking for $\tau P = 0.067$, $\phi = 0.46$, and $C_s = -0.13$. Blockage for $\tau P = 0.095$ and $\phi = 0.46$. C_s is not defined because of blocking.

We may examine how they were correlated by measuring the cross association between the upper and lower interface curves. This makes it easier to discern between a form of meandering and a type of deposition necking. Cross correlation is described as

$$C_c = \left\langle \frac{Cov(h_1, h_2)}{\sigma_1 \sigma_2} \right\rangle$$

$$Cov(h_1, h_2) = n^{-1} \sum_i (h_1(x, t) - \bar{h}_1(t)) (h_2(x, t) - \bar{h}_2(t))$$

$$\sigma_\alpha^2 = n^{-1} \sum_i (h_\alpha(x, t) - \bar{h}_\alpha(t))^2$$

Where σ the standard deviation, n is the number of points at the interface curves, $\alpha = 1, 2$ refers to the upper and lower interfaces, respectively, the bar denotes average over an interface, and the angular brackets denote ensemble average. There was an exception at $\phi \approx 0.38$, where the intermediate region between the onset of deposition and blocking was very narrow. As τP approached the blocking limit $\tau P = \tau_b$, cross correlation typically became negative, i.e. the interfaces at opposite sides of the channel were anti-correlated. This suggests a flow path necking action. Fluctuations can most likely push the two interfaces together in this situation, so that the flow path tends to be completely blocked (Figure 1). However the precise step boundary between the meandering type and the necking type of behaviour is difficult to ascertain owing to significant fluctuations.

However, by numerically calculating the approximate positions of three-phase borders, we could create the phase diagram and justify them by semi-analytical arguments [V]. It was difficult to establish the potential step boundary between meandering and necking forms of flow paths even numerically, but we also have an approximation for that boundary based on cross-correlations (assuming it exists).

The phase diagram and approximate projections for three phase limits are seen in fig 2.

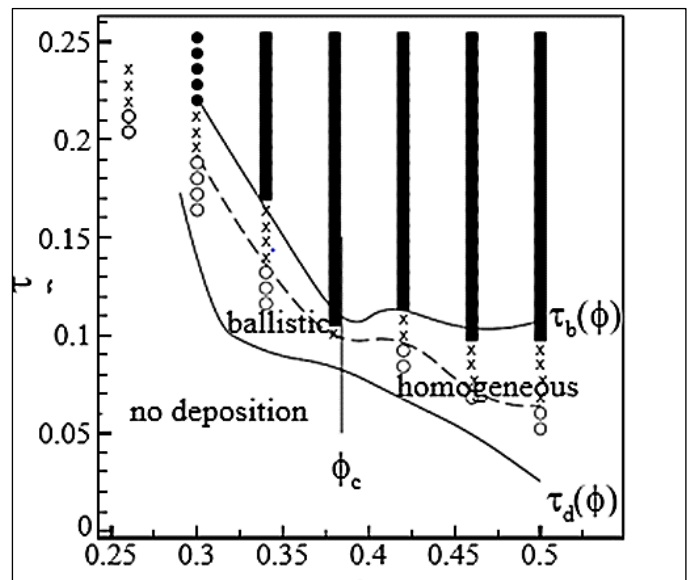


Fig 2: A generic phase diagram that describes the location of six phases in the $(\tau P, \phi)$ space. (•) Full blocking, (x) deposition layers with necking, $C_s < 0$, and (o) deposition layers with meandering, $C_s \geq 0$.

In the phase with deposition layers at low ϕ and high τP , there was no detachment of particles, and columns of particles typical of ballistic deposition without relaxation were formed [10, 11]. At high ϕ and low τP , the structure was characterised by rapid attachment and detachment events, which culminated in more or less homogeneous and thick layers of deposited particles following extensive rearrangements. Unlike in the case of ballistic deposition, the density in the deposited layer was greater than in the suspension, and the deposited layer thickness rose before detachment and attachment events were balanced (fig 3).

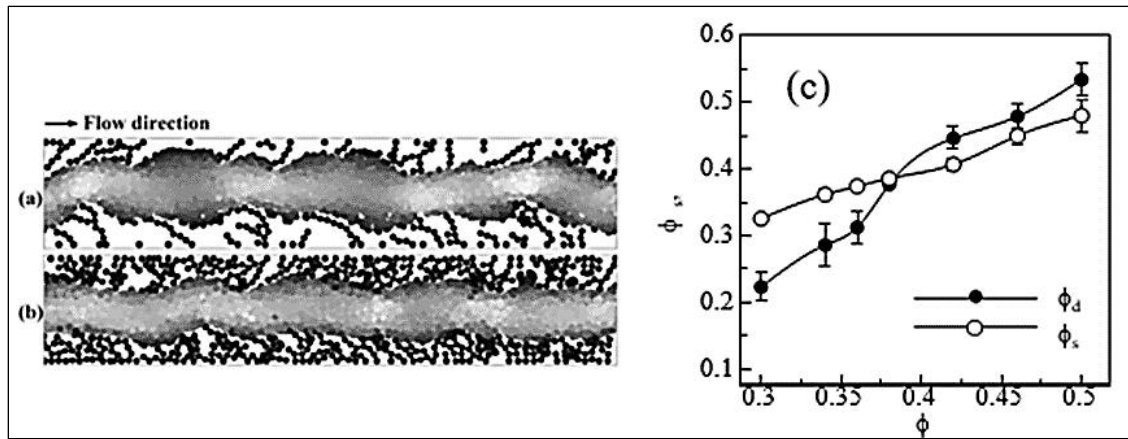


Fig 3: Superimposed snapshots with grey scale coded particle velocities regardless of fluid contours (white is high particle velocity and black is zero particle velocity). Ballistic type of deposition, $\tau P = 0.14$, $\phi = 0.3$, and $\phi_d / \phi_s \approx 0.76$. (b) Dense and homogeneous deposition layers for $\tau P = 0.053$, $\phi = 0.5$, and $\phi_d / \phi_s \approx 1.15$. (c) The average concentration of particles in the deposited layers ϕ_d and the concentration of suspended particles in the flow channel ϕ_s , as functions of the solid volume fraction ϕ for $\tau P = 0.1$.

We have considered the existence of fluctuations in the interfaces in order to further analyse the clogging transition. It is apparent that in the deposited soils, hydrodynamic drag forces are highest near the local limit and that they are lowest near the local minimum. There is no mechanism in the device that would move the interface locally in the usual direction, nor is there any direct diffusion in the layers deposited. Therefore, we do not assume nonlinear terms to occur in this equation, such as the one in the equation of Kardar-Parisi-Zhang [12-14]

Conclusion

Numerical methods were used in the present research to explore many phenomena of fluid flow. Microscale MD simulations of solid particles and mesoscopic LB simulations of liquid-particle suspensions have been tested in both single- and multi-phase structures. The decay of diffusion coefficients along with changes from disordered to layered structures was observed in molecular dynamics simulations of dense, monosized, rugged inelastic particles, and the diffusion coefficients were also studied as shear rate functions. In order to find out whether the method can be used to simulate fluid imbibition in porous media, we tested the use of the lattice-Boltzmann method in studying the classical capillary rise problem. The findings were positive and demonstrated the well-known activity of capillary rise, but due to discretization issues, only for large capillary radii. A liquid-particle suspension pipe flow was also considered, in which the deposition of particles on the pipe walls, along with the isolation of deposited particles for sufficiently high hydrodynamic forces, was permitted. A rich phase diagram for this method was seen to cover two factors, solid volume fraction and detachment threshold. For a variety of fascinating and important applications in industrial as well as biological flow problems, these findings are expected to be a starting point.

References

1. Zuriguel DR, Parisi RC, Hidalgo C, Lozano A, Janda PA, Gago JP. *Clément et al.*, *Sci. Rep* 2014;4:7324.
2. Beverloo WA, Leniger HA, Van de Velde J, *Chem. Eng. Sci* 1961;15:260.
3. Kulkarni SD, Metzger B, Morris JF. *Phys. Rev* 2010;82:010402.

4. Xi. Wu, Maloy KJ, Hansen A, Ammi M, Bideau D. *Phys. Rev. Lett* 1993;71:1363.
5. Sharp KV, Adrian RJ, *Microfluid. Nanofluid* 2005;1:376.
6. Singh P, Venkatesan R, Fogler HS, Nagarajan NR *AIChE J* 2001;47:6.
7. Imbesi SG, Kerber W, *AJNT Am. J Neuroradiol* 1998;19:761.
8. Meakin P, Sun T, Jossang T, Schwarz K. *Physica A* 1996;233:606.
9. Edwards BF, Smith DH *Phys. Rev. E* 2002;65:046303.
10. Ramanlal P, Sander LM. *Phys. Rev. Lett* 1985;54:1828.
11. Krug J, *Materialwissenschaft und Werkstofftechnik* 1995;26:22.
12. Kardar M, Parisi G, Zhang YC. *Phys. Rev. Lett* 1986;56:889.
13. Villain J, *J Phys* 1991;I(1):19.
14. Edwards SF, Wilkinson DR, *Proc. R. Soc. London, Ser. A* 1982;381:17.